Pnicogen-Bonded Complexes HnF5-nP:N-Base, for n=0-5

ARTICLE *in* THE JOURNAL OF PHYSICAL CHEMISTRY A · OCTOBER 2014

Impact Factor: 2.69 · DOI: 10.1021/jp509353a · Source: PubMed

3 AUTHORS, INCLUDING:

Ibon Alkorta
Spanish National Research Council
680 PUBLICATIONS **12,430** CITATIONS
SEE PROFILE

José Elguero
Spanish National Research Council
1,502 PUBLICATIONS **22,206** CITATIONS
SEE PROFILE

THE JOURNAL OF PHYSICAL CHEMISTRY A

Article

pubs.acs.org/JPCA

Pnicogen-Bonded Complexes $H_nF_{5-n}P$:N-Base, for n = 0−5

Janet E. Del Bene,*[,†] Ibon Alkorta,*[,‡] and José Elguero[‡]

[†]Department of Chemistry, Youngstown State University, Youngstown, Ohio 44555, United States

[‡]Instituto de Química Médica (IQM-CSIC), Juan de la Cierva, 3, E-28006 Madrid, Spain

Supporting Information

ABSTRACT: Ab initio MP2/aug′-cc-pVTZ calculations have been carried out on the pnicogen-bonded complexes $H_nF_{5-n}P$:N-base, for n = 0−5 and nitrogen bases NC^-, NCLi, NP, NCH, and NCF. The structures of these complexes have either C_{4v} or C_{2v} symmetry with one exception. P−N distances and interaction energies vary dramatically in these complexes, while F_{ax}−P−F_{eq} angles in complexes with PF_5 vary from 91° at short P−N distances to 100° at long distances. The value of this angle approaches the F_{ax}−P−F_{eq} angle of 102° computed for the Berry pseudorotation transition structure which interconverts axial and equatorial F atoms of PF_5. The computed distances and F_{ax}−P−F_{eq} angles in complexes F_5P:N-base are consistent with experimental CSD data. For a fixed acid, interaction energies decrease in the order NC^- > NCLi > NP > NCH > NCF. In contrast, for a fixed base, there is no single pattern for the variations in distances and interaction energies as a function of the acid. This suggests that there are multiple factors that influence these properties. The dominant factor appears to be the number of F atoms in equatorial positions, and then a linear F_{ax}−P···N rather than H_{ax}−P···N alignment. The acids may be grouped into pairs (PF_5, PHF_4) with four equatorial F atoms, then (PH_4F, PH_2F_3) with F_{ax}−P···N linear, and then (PH_3F_2 and PH_5) with H_{ax}−P···N linear. The electron-donating ability of the base is also a factor in determining the structures and interaction energies of these complexes. Charge transfer from the N lone pair to the σ^* P−A_{ax} orbital stabilizes $H_nF_{5-n}P$:N-base complexes, with A_{ax} either F_{ax} or H_{ax}. The total charge-transfer energies correlate with the interaction energies of these complexes. Spin−spin coupling constants ^{1p}J(P−N) for (PF_5, PHF_4) complexes with nitrogen bases are negative with the strongest bases NC^- and NCLi but positive for the remaining bases. Complexes of (PH_4F, PH_2F_3) with these same two strong bases and H_4FP:NP have positive ^{1p}J(P−N) values but negative values for the remaining bases. (PH_5, PH_3F_2) have negative values of ^{1p}J(P−N) only for complexes with NC^-. Values of ^1J(P−F_{ax}) and ^1J(P−H_{ax}) correlate with the P−F_{ax} and P−H_{ax} distances, respectively.

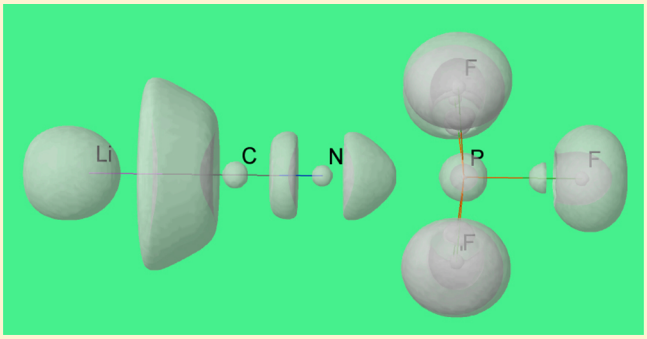

INTRODUCTION

The pnicogen bond is one of the newer members of the family of intermolecular interactions. This bond arises when a pnicogen atom acts as an electron-pair acceptor in a Lewis acid−Lewis base interaction. While the pnicogen bond had been recognized for some time,[1−6] it was not until 2011 that this bond became the subject of intense interest,[7,8] as evident from the number of papers published on the pnicogen bond since that time.[9−45] Most of these studies have examined complexes involving PH_3 and its derivatives, although there have been a few studies of complexes containing derivatives of $H_2C{=}PH$ and $HC{\equiv}P$. Pnicogen bonding occurs as electrons are donated to P through its σ-hole in the saturated molecules, and through its σ- or π-hole in the unsaturated molecules.[46−48]

There have been two theoretical studies of pnicogen bonds involving higher valence states of phosphorus, one on phosphine oxide derivatives[49] and the other on a complex of PF_5 with pyridine.[50] To what extent can these higher valence states of phosphorus engage in pnicogen bonding, and what are the properties of the resulting complexes? To answer these questions, we have examined a series of pnicogen-bonded complexes in which the Lewis acids are PH_nF_{5-n} for n = 0−5 and the nitrogen bases are NC^-, NCLi, NP, NCH, and NCF. These complexes have a distorted octahedral environment with either C_{4v} or C_{2v} symmetry, except for H_3F_2P:NP which has C_s symmetry. We have determined the structures and interaction energies of these complexes, their bonding properties, and spin−spin coupling constants ^{1p}J(P−N), ^1J(P−F_{ax}), and ^1J(P−H_{ax}), with F_{ax} and H_{ax} the axial atoms bonded to P. In this paper we present the results of this investigation.

METHODS

The structures of the isolated bases and the complexes $H_nF_{5-n}P$:N-base were optimized at second-order Møller−Plesset perturbation theory (MP2)[51−54] with the aug′-cc-pVTZ basis set.[55] This basis set is derived from the Dunning aug-cc-pVTZ basis set by removing diffuse functions from H

Received: September 15, 2014
Revised: September 29, 2014
Published: October 20, 2014

   dx.doi.org/10.1021/jp509353a | J. Phys. Chem. A 2014, 118, 10144−10154

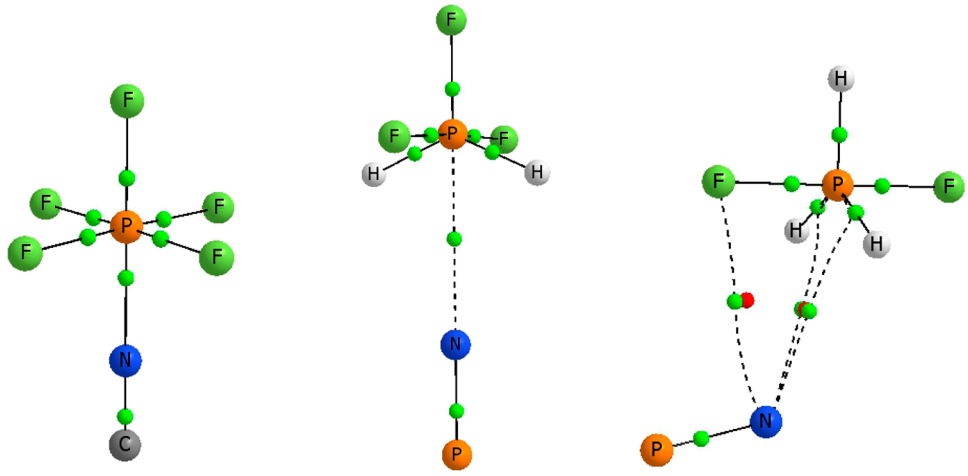

Figure 1. Complexes $H_5P{:}NC^-$ (C_{4v}), $H_2F_3P{:}NP$ (C_{2v}), and $PH_3F_2{:}NP$ (C_s).

atoms.[56,57] Frequencies were computed to establish that the optimized structures correspond to equilibrium structures on their potential surfaces. Optimization and frequency calculations were performed using the Gaussian 09 program.[58]

Even though the distorted octahedral complexes reported in this paper are equilibrium structures on their potential surfaces, some complexes are not bound relative to the nitrogen base and an isolated PH_nF_{5-n} molecule which has a trigonal bipyramidal or a distorted trigonal bipyramidal structure. Therefore, instead of computing binding energies, we have computed interaction energies as the difference between the total energy of the complex and the energies of the corresponding monomers PH_nF_{5-n} and N-base, with the monomers at their geometries in the complex.

The electron densities of the complexes have been analyzed using the atoms in molecules (AIM) methodology[59−62] and the electron localization function (ELF),[63] employing the AIMAll[64] and TopMod[65] programs. The topological analysis of the electron density produces the molecular graph of each complex. This graph identifies the location of electron density features of interest, including the electron density (ρ) maxima associated with the various nuclei, saddle points which correspond to bond critical points (BCPs), and ring critical points which indicate a minimum electron density within a ring. The zero gradient line which connects a BCP with two nuclei is the bond path. The electron density at the BCP (ρ_{BCP}), the Laplacian of the electron density at the BCP ($\nabla^2\rho_{BCP}$), and the total energy density (H_{BCP}) are additional useful quantities for characterizing interactions.[66]

Natural bond order (NBO)[67] MP2/aug′-cc-pVTZ electron populations have been evaluated for all complexes. In addition, the NBO method has been used to analyze the stabilizing charge-transfer interactions using the NBO-6 program.[68] Because MP2 orbitals are nonexistent, the charge-transfer interactions have been computed using the B3LYP functional[69,70] with the aug′-cc-pVTZ basis set at the MP2/aug′-cc-pVTZ complex geometries, so that at least some electron correlation effects could be included.

Spin−spin coupling constants were evaluated using the equation-of-motion coupled cluster singles and doubles (EOM-CCSD) method in the CI (configuration interaction)-like approximation,[71,72] with all electrons correlated. For these calculations, the Ahlrichs[73] qzp basis set was placed on ^{13}C, ^{15}N, and ^{19}F, and the qz2p basis set on ^{31}P and axial ^{1}H atoms. The Dunning cc-pVDZ basis set was placed on the remaining hydrogens. A previously developed basis set which contains the same number of functions as the qzp basis was placed on ^{7}Li atoms.[74] The EOM-CCSD calculations were performed using ACES II[75] on the IBM Cluster 1350 (Glenn) at the Ohio Supercomputer Center.

RESULTS AND DISCUSSION

Monomers. The structure of PF_5 is known experimentally to have equatorial and axial P−F bond lengths of 1.577 ± 0.005 and 1.534 ± 0.004 Å, respectively.[76] The computed P−F distances are about 0.015 Å longer than the experimental distances, but both experimental and computed values indicate that the axial P−F bonds are about 0.04 Å shorter than the equatorial bonds. In addition, an electron diffraction study of $P(CH_3)_2F_3$ reported $P-F_{ax}$ and $P-F_{eq}$ bonds lengths of 1.643 ± 0.003 and 1.553 ± 0.006 Å, respectively.[76] The corresponding computed P−F bond lengths for PH_2F_3 are 1.635 and 1.562 Å, respectively.

The PH_nF_{5-n} molecules have trigonal bipyramidal or slightly distorted trigonal bipyramidal structures. The molecular electrostatic potentials of PF_5 and PH_5 exhibit σ-holes with values of +0.051 and +0.026 au, respectively. However, the σ-holes are rather unfavorable for interaction of a base with P in PF_5 because the holes are located between F atoms. An electron diffraction study of the PF_5 molecule[76] revealed a trigonal bipyramidal structure of D_{3h} symmetry. However, the nuclear magnetic resonance spectrum of this molecule has only one fluorine resonance, which indicates a low barrier for interconversion of the axial and equatorial fluorines.[77,78] The Berry pseudorotation mechanism,[79] which involves a transition structure of C_{4v} symmetry, has been proposed as the reason for such a low barrier.[80−88] Therefore, we have optimized the C_{4v} transition structures of PF_5 and PH_5 and have determined that the barriers for interconversion of axial and equatorial atoms are 17.4 and 8.2 kJ·mol^{-1}, respectively. The transition structures also have σ-holes much larger than those of the equilibrium structures, with values of +0.106 and +0.052 au, respectively. The σ-hole is found at P on the C_4 axis on the opposite side of the $P-F_{ax}$ or $P-H_{ax}$ bond. This is the site of complex formation with the nitrogen bases, which have negative MEPs of −0.285, −0.126, −0.066, −0.066, and −0.057 au for NC^-, NCLi, NP, NCH, and NCF, respectively.

dx.doi.org/10.1021/jp509353a | J. Phys. Chem. A 2014, 118, 10144−10154

Interaction Energies and Geometries of Complexes $H_nF_{5-n}P$:N-Base. Table S1 of the Supporting Information reports the structures, total energies, and electron density molecular graphs of complexes $H_nF_{5-n}P$:N-base, and Figure 1 illustrates the structures and molecular graphs of H_5P:NC^- (C_{4v}), H_2F_3P:NP (C_{2v}), and PH_3F_2:NP (C_s). All of the complexes with PF_5, PHF_4, PH_4F, and PH_5 have C_{4v} symmetry, which is the same symmetry as that of the Berry transition structures of the monomers which lead to the exchange of axial and equatorial atoms.

The computed interaction energies of all complexes are listed in Table 1, and the intermolecular P−N distances are reported in Table 2. The interaction energies of neutral complexes span a large range, from −13 kJ·mol^{-1} for H_3F_2P:NCF to −193 kJ·mol^{-1} for F_5P:NCLi. This range is extended to −391 kJ·mol^{-1} when the anionic complexes are included. For a fixed acid as a function of the base, interaction energies exhibit an exponential dependence on the P−N distance, with correlation coefficients R^2 of 0.929 or greater. Quadratic correlations between interaction energies and P−N distances have slightly better correlation coefficients, but the trendlines have incorrect curvature at long distances. With a fixed Lewis acid, the interaction energies decrease in the expected order with respect to the base, namely NC^- > NCLi > NP > NCH > NCF.

Table 1. MP2/aug′-cc-pVTZ Interaction Energies (ΔE, kJ·mol^{-1}) for Complexes $H_nF_{5-n}P$:N-Base

acid/base	NC^-	NCLi	NP	NCH	NCF
PF_5	−391.1	−192.6	−108.9	−62.2	−43.0
PHF_4	−355.9	−169.8	−89.4	−35.8	−29.1
PH_2F_3	−255.2	−82.6	−25.1	−21.7	−20.4
PH_3F_2	−146.0	−25.3	−16.3[a]	−13.7	−13.2
PH_4F	−242.3	−107.8	−65.5	−48.5	−42.9[b]
PH_5	−93.4	−30.8	−19.9	−16.1	−15.3

[a]The equilibrium structure with C_s symmetry. The complex with C_{2v} symmetry has a similar interaction energy of −15.3 kJ·mol^{-1}. [b]The complex of C_{2v} symmetry which has one imaginary frequency.

Table 2. MP2/aug′-cc-pVTZ P−N Distances [R(P−N), Å] in Complexes $H_nF_{5-n}P$:N-Base

acid/base	NC^-	NCLi	NP	NCH	NCF
PF_5	1.796	1.902	2.016	2.239	2.452
PHF_4	1.802	1.912	2.052	2.499	2.632
PH_2F_3	1.878	2.183	2.906	2.995	3.010
PH_3F_2	1.995	3.084	3.220[a]	3.243	3.241
PH_4F	1.892	2.050	2.161	2.299	2.356
PH_5	2.118	2.615	2.768	2.872	2.891

[a]The equilibrium complex with C_s symmetry. The C_{2v} complex has a P−N distance of 3.241 Å.

What is more interesting and challenging to understand is the variation of interaction energies with the P−N distance for a fixed base as a function of the acid. The lack of a single pattern suggests that there must be several factors which influence these energies. These include the atoms involved in the linear arrangement across the pnicogen bond, F_{ax}−P···N or H_{ax}−P···N; the number of F atoms bonded to P in equatorial positions; and the electron-donating ability of the base. To obtain some insight into the relative interaction energies of the acids, it is advantageous to group them into pairs, based first on the number of F atoms in equatorial positions and second on whether the linear arrangement across the pnicogen bond is F_{ax}−P···N or H_{ax}−P···N.

Complexes of the acids PF_5 and PHF_4 have the largest interaction energies with the three strongest bases NC^-, NCLi, and NP. These complexes have an equatorial plane containing four F atoms that withdraw electron density from P, making that atom a better electron-pair acceptor for the formation of a pnicogen bond. F_5P:N-base has a greater interaction energy than HF_4P:N-base with each nitrogen base because complexes with PF_5 also have F_{ax}−P···N linear, while those with PHF_4 have H_{ax}−P···N linear. That F−P···P linear has a greater stabilizing effect than H−P···P linear has been observed in previous studies of pnicogen bonds.[11,12]

When the complexes with the stronger bases NC^-, NCLi, and NP are compared, the complexes which are next in stability are those with PH_2F_3 and PH_4F as the acids. H_2F_3P:NC^- has an interaction energy greater than that of H_4FP:NC^-, but the complexes of PH_4F with NCLi and NP have interaction energies greater than those with PH_2F_3. Both sets of complexes have F_{ax}−P···N linear, but differ insofar as PH_2F_3 has two equatorial F atoms while PH_4F has none. Complexes of PH_3F_2 and PH_5 also have two and zero equatorial F atoms, respectively, but have the weakest interaction energies with all bases. This may be attributed to the linear H_{ax}−P···N alignment in these complexes. These comparisons suggests that for a fixed strong base, having four F atoms in the equatorial plane is the dominant factor in determining the interaction energies, but the F_{ax}−P···N alignment is more important than having zero or two F atoms in the plane and much more significant than having H_{ax}−P···N linear. For these pairs of acids with the stronger bases, the order of decreasing binding energies is (PF_5, PHF_4) > (PH_4F, PH_2F_3) > (PH_5, PH_3F_2).

From Table 1 it can also be seen that there are changes in the above order as the bases becomes weaker and thus poorer electron-pair donors. For example, the interaction energy of F_5P:NC^- is 149 kJ·mol^{-1} greater than that of H_4FP:NC^-, but the difference in interaction energies decreases as the base strength decreases until the complexes of these two acids with NCF have the same interaction energies. With the weaker bases NCH and NCF, complexes of PH_4F have interaction energies greater than those with PHF_4, which suggests that for these complexes, having F_{ax}−P···N linear is more important than having four fluorines in the equatorial plane.

The variation of the interaction energies with the P−N distances is illustrated in Figure 2. From this figure, it is possible to make some generalizations about the strength of the interactions involving the PH_nF_{5-n} acids. Using a P−N distance of 2.65 Å and an interaction energy of −29 kJ·mol^{-1} as a reference, it can be seen that all complexes with PF_5, PHF_4, and PH_4F have shorter P−N distances and interaction energies of −29 kJ·mol^{-1} or greater. In contrast, complexes of the acids PH_2F_3 and PH_5 have shorter distances and greater interaction energies only with the strong bases NC^- and NCLi. The only complex of PH_3F_2 with a shorter distance and greater interaction energy is the anionic complex. From Figure 2 it is evident that the latter three acids do not discriminate among the weaker bases.

In the complexes with the acids PF_5 and PHF_4, the N−P−F_{eq} angles and therefore the A_{ax}−P−F_{eq} angles vary with the P−N distance, as illustrated in Figure 3, with A the axial F or H atom. The correlation coefficients for the second-order trendlines are

dx.doi.org/10.1021/jp509353a | J. Phys. Chem. A 2014, 118, 10144−10154

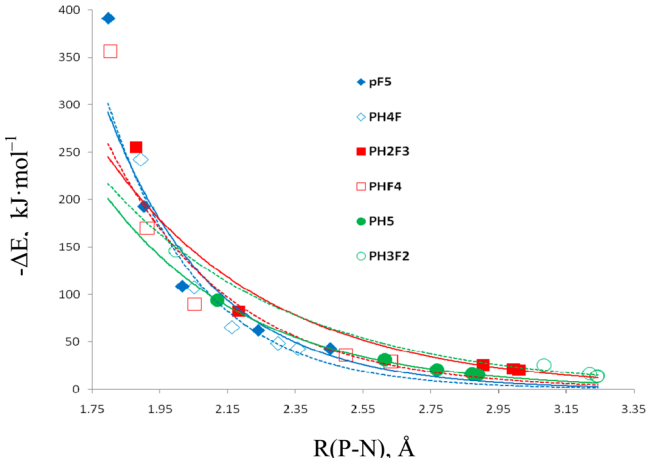

Figure 2. Negative of the interaction energies ($-\Delta E$) versus the P−N distances for complexes $H_nF_{5-n}P$:N-base.

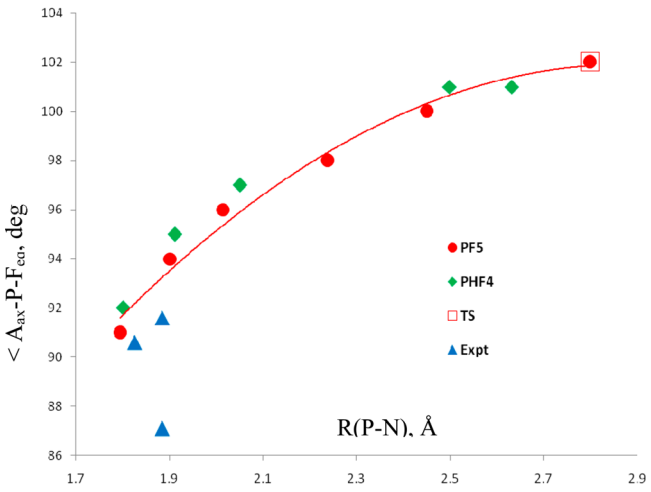

Figure 3. Angles $A_{ax}-P-F_{eq}$ versus the P−N distance for complexes F_5P:N-base and HF_4P:N-base with A_{ax} either F_{ax} or H_{ax}. Experimental data are $F_{ax}-P-F_{eq}$ angles from the CSD for complexes between PF_5 and nitrogen bases.

0.986 and 0.996, respectively. However, the $A_{ax}-P-F_{eq}$ angles in complexes with PH_3F_2 and PH_2F_3 show little dependence on the P−N distance because these angles vary by only 3° over a wide range of distances. Also shown in Figure 3 are experimental P−N distances and $F_{ax}-P-F_{eq}$ angles taken from the CSD database[89] for three complexes involving PF_5 and nitrogen bases. These complexes are identified in Scheme S1 of the Supporting Information. It is evident that the computed structures are consistent with the experimental values. Moreover, Figure 3 indicates that the $F_{ax}-P-F_{eq}$ angle is 91° at a P−N distance of 1.796 Å in the complex with the strongest base NC^- but increases to 100° at a P−N distance of 2.452 Å in the complex with the weakest base NCF. The computed value of the $F_{ax}-P-F_{eq}$ angle in the PF_5 transition structure with C_{4v} symmetry is 102°. The point for the transition structure is shown in Figure 3 at a P−N distance of 2.8 Å, which is assumed to be a distance at which stable complexes are unlikely. Thus, the values of the $F_{ax}-P-F_{eq}$ angle in complexes F_5P:N-base converge with increasing P−N distance to the value of this angle in the Berry transition structure.

AIM, NBO, and ELF Results. Charge transfer has been demonstrated to be an important factor in the stabilization of pnicogen-bonded complexes. In the $H_nF_{5-n}P$:N-base complexes, charge transfer occurs from the N lone pair of the base to the antibonding σ^* P−A_{ax} orbital of the acid, where A is the axial F or H atom. In addition, complexes of PF_5 and PHF_4 have four other charge-transfer interactions, from the N lone pair of the base to each of the antibonding σ^* P−F_{eq} orbitals. Table 3 reports the charge-transfer energies for these complexes.

The NBO program treats as single molecules the complexes of NC^- that have either four equatorial F atoms or $F_{ax}-P-N$ linear, and those of PF_5 with the stronger bases NCLi and NP. Of those that remain, the complexes of PF_5, PHF_4, and PH_4F have N(lp) → σ^*P−A_{ax} charge-transfer energies ranging from 11 to 129 kJ·mol^{-1}. In addition, complexes with four equatorial F atoms have four N(lp) → σ^*P−F_{eq} charge-transfer energies which impart additional stability. These complexes and the complexes of PH_2F_3 and PH_5 with the strong base NCLi have total charge-transfer energies which range from 40 to 455 kJ·mol^{-1}. In contrast, except for H_2F_3P:NCLi, neutral complexes with two F atoms in equatorial positions have charge-transfer energies less than 8 kJ·mol^{-1}. Total charge-transfer energies and interaction energies are linearly related, with a correlation coefficient R^2 of 0.931.

Table 4 reports the NBO MP2/aug′-cc-pVTZ charges on PH_nF_{5-n} in the complexes $H_nF_{5-n}P$:N-base. As anticipated,

Table 4. NBO MP2/aug′-cc-pVTZ Charges (au) on PH_nF_{5-n} in Complexes $H_nF_{5-n}P$:N-Base

acid/base	NC^-	NCLi	NP	NCH	NCF
PF_5	−0.364	−0.261	−0.188	−0.099	−0.047
PHF_4	−0.375	−0.264	−0.177	−0.043	−0.026
PH_2F_3	−0.325	−0.145	−0.011	−0.006	−0.006
PH_3F_2	−0.272	−0.005	−0.003	−0.002	−0.002
PH_4F	−0.329	−0.206	−0.141	−0.099	−0.082
PH_5	−0.224	−0.054	−0.031	−0.020	−0.019

Table 3. Charge-Transfer Energies [N(lp) → σ^*P−A_{ax} and N(lp) → σ^*P−F_{eq}, kJ·mol^{-1}] for Complexes $H_nF_{5-n}P$:N-Base[a]

acid/base	NC^-	NCLi	NP	NCH	NCF
PF_5	*b*	*b*	*b*	61.5 (18.8)	57.7 (9.6)
PHF_4	*b*	128.9 (81.6)	70.7 (45.6)	17.2 (10.0)	11.3 (5.9)
PH_2F_3	*b*	102.5	7.9	5.9	5.9
PH_3F_2	162.8 (23.8)[c]	5.4	2.9	2.9	2.9
PH_4F	*b*	189.5	123.8	90.8	78.2
PH_5	164.8	40.2	22.6	17.2	17.6

[a]Values in parentheses are N(lp) → σ^*P−F_{eq} charge-transfer energies for each P−F_{eq} bond. [b]The NBO program treats this complex as a single molecule. [c]There are also two N(lp) → σ^*P−H_{eq} charge-transfer energies of 69.5 kJ·mol^{-1}.

dx.doi.org/10.1021/jp509353a | J. Phys. Chem. A 2014, 118, 10144−10154

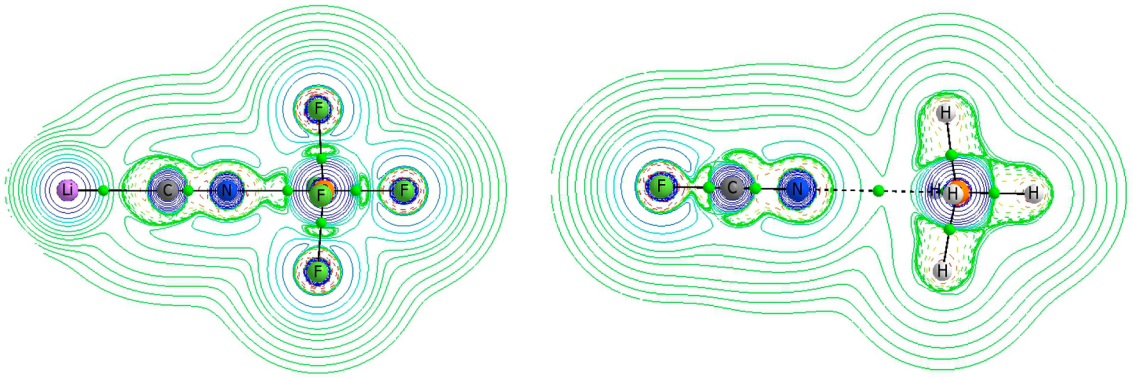

Figure 4. Laplacian contours for (a) F_5P:NCLi and (b) H_5P:NCF. Positive and negative values of the Laplacians are represented as solid and dashed lines, respectively.

these charges are very large when the base is the anion NC^-, with values ranging from −0.224 to −0.375e. Not surprisingly, the complexes identified above as having large charge-transfer energies also have greater negative charges on PH_nF_{5-n} molecules. Neutral complexes with two F atoms in equatorial positions except for H_2F_3P:NCLi have charges on the acids of −0.011e or less.

The electron density at the bond critical point (ρ_{BCP}), the Laplacian of the electron density at the BCP ($\nabla^2\rho_{BCP}$), and the total energy density at that point (H_{BCP}) for complexes $H_nF_{5-n}P$:N-base are reported in Tables S2, S3, and S4, respectively, of the Supporting Information. As is usually the case, electron densities at bond critical points correlate exponentially with P−N distances, with a correlation coefficient R^2 of 0.992.[90−98] The Laplacians of the electron densities are always positive and show an interesting distance dependence. The value of the Laplacian decreases dramatically from 0.244 to 0.012 for the anionic complexes and several of the more strongly interacting complexes with NCLi and NP. Subsequently, the values of the Laplacian increase slightly and then oscillate as the P−N distance increases and the bonds become weak intermolecular bonds. This pattern is typical of weak intermolecular interactions such as hydrogen bonds.[99,100] Although the Laplacians for all complexes $H_nF_{5-n}P$:N-base are positive, the Laplacian contours in the intermolecular region of F_5P:NCLi and F_5P:NCF in panels a and b of Figure 4, respectively, illustrate significant differences between them. For the strongly interacting F_5P:NCLi complex which has a short P−N distance, negative Laplacian contours are located in the intermolecular region between P and N. While the BCP is close to the negative region, it is actually located in the positive region near P, resulting in a positive value for the Laplacian of the electron density at the BCP. In contrast, in the weakly interacting complex F_5P:NCF with a long P−F distance, the intermolecular region has positive Laplacian contours and also a positive value of the Laplacian at the BCP.

Most interesting is the behavior of the energy densities at the BCPs of these complexes, which is illustrated in Figure 5. All complexes with PF_5, PHF_4, and PH_4F have negative values of the energy densities at bond critical bonds, again indicating that the P···N bonds in these complexes have some covalent character. Complexes of PH_2F_3 and PH_5 have negative values of the energy density only with the strong bases NC^- and NCLi. The only complex of PH_3F_2 which has a negative energy

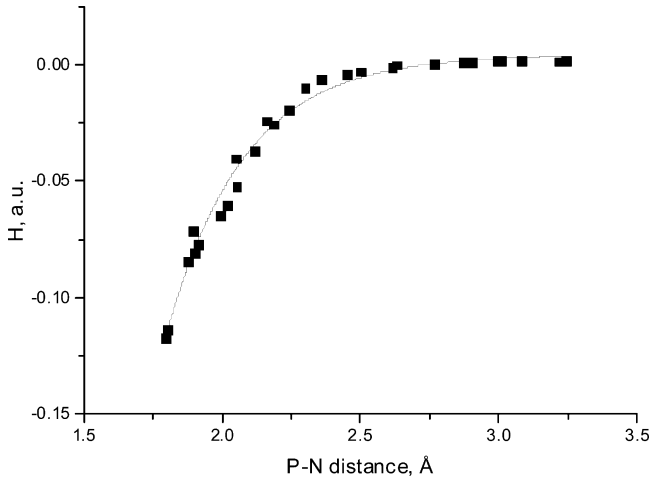

Figure 5. Energy density at the BCP versus the P−N distance for complexes $H_nP_{5-n}P$:N-base. The fitted asymptotic equation has an R^2 value of 0.99.

density at the BCP is H_3F_2P:NC^-. These five complexes also have P···N bonds with partial covalent character. These same complexes were identified as having P−N distances less than 2.65 Å and interaction energies greater than −29 kJ·mol^{-1}.

ELF isosurfaces of F_5P:NCLi and F_5P:NCF are shown in panels a and b of Figure 6, respectively. In both complexes, ELF basins correspond to the nitrogen lone pairs clearly pointing toward the phosphorus atoms. In the complex F_5P:NCF, the nitrogen base is a weak electron-pair donor, and the F_{ax}−P−F_{eq} angles approach the value in the C_{4v} Berry pseudorotation transition structure for PF_5. In contrast, in the F_5P:NCLi complex with the much stronger electron-donating base, the F_{ax}−P−F_{eq} angles decrease to reduce the repulsion between the nitrogen lone pair and the equatorial F atoms.

Spin−Spin Coupling Constants. Components of spin−spin coupling constants ^{1p}J(P−N), ^1J(P−F_{ax}), and ^1J(P−H_{ax}) are reported in Tables S5 and S6 of the Supporting Information. These data indicate that ^{1p}J(P−N) and ^1J(P−H_{ax}) are dominated by the FC terms, which are excellent approximations to total J. Although the FC terms are also the dominant contributors to ^1J(P−F_{ax}), they are not good approximations to these coupling constants owing to non-negligible contributions from the PSO and SD terms.

dx.doi.org/10.1021/jp509353a | J. Phys. Chem. A 2014, 118, 10144−10154

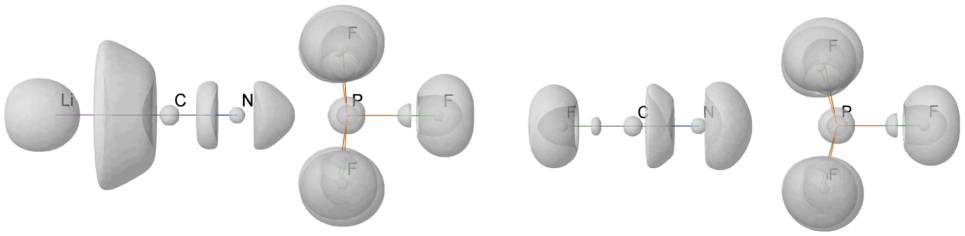

a b

Figure 6. ELF 0.8 isosurfaces of (a) F_5P:NCLi and (b) F_5P:NCF.

^{1p}J(P−N) values for the complexes $H_nF_{5-n}P$:N-base are reported in Table 5. The values for the anionic complexes span

Table 5. Coupling Constants [^{1p}J(P−N), Hz] for Complexes $H_nF_{5-n}P$:N-Base

acid/base	NC^-	NCLi	NP	NCH	NCF
PF_5	−58.8	−25.2	3.8	14.3	12.4
PHF_4	−57.0	−19.4	12.9	13.4	10.2
PH_2F_3	58.1	47.0	−18.8	−17.8	−18.9
PH_3F_2	74.2	−16.7	−9.1[a]	−11.9	−12.5
PH_4F	46.8	37.5	13.9	−1.7	−10.0
PH_5	52.7	−1.2	−7.5	−7.5	−8.3

[a]The equilibrium complex with C_s symmetry. The C_{2v} complex has ^{1p}J(P−N) = −12.8.

a wide range, from −58 Hz for F_5P:NC^- and HF_4P:NC^- to +74 Hz for PH_3F_2:NC^-. Coupling constants for neutral complexes may also be either positive or negative, ranging from −25 Hz for F_5P:NCLi to +47 Hz for H_2F_3P:NCLi. It is apparent from Table 5 that these coupling constants follow a pattern which reflects the grouping of acids presented above. Complexes with PF_5 and PHF_4 have negative coupling constants with NC^- and NCLi and positive values with the remaining bases. Complexes with PH_2F_3 and PH_4F have positive coupling constants with the bases NC^- and NCLi, and H_4FP:NP also has a positive ^{1p}J(P−N). All of the remaining complexes with these acids have negative ^{1p}J(P−N) values. Complexes of PH_3F_2 and PH_5 have positive coupling constants only when NC^- is the base.

Figure 7 presents a plot of ^{1p}J(P−N) versus the P−N distance for complexes F_5P:N-base and HF_4P:N-base, which have four F atoms in the equatorial plane. These coupling constants do not distinguish well between the weak bases NCH and NCF, and PHF_4 with NP, because ^{1p}J(P−N) values for these complexes lie between 10 and 14 Hz over a wide range of P−N distances from 2.05 to 2.63 Å. However, ^{1p}J(P−N) decreases to 4 Hz for F_5P:NP at a distance of 2.02 Å. At a distance of about 1.9 Å, ^{1p}J(P−N) values become −19 and −25 Hz for HF_4P:NCLi and F_5P:NCLi, respectively. A further decrease in the distance to about 1.80 Å leads to ^{1p}J(P−N) values of about −58 Hz for the two complexes with NC^-. The second-order curve shown in Figure 7 refers to all of the complexes and has a correlation coefficient of 0.941, but it does not describe ^{1p}J(P−N) at distances of 2.05 Å or greater.

The values of the P−N distances in the anionic complexes with PF_5 and PHF_4 are approaching the computed values of the P−N distances in the molecules F_2PNC and H_2PNC, which are 1.726 and 1.720 Å, respectively. However, ^1J(P−N) for these two molecules are positive with computed values of 62 and 91

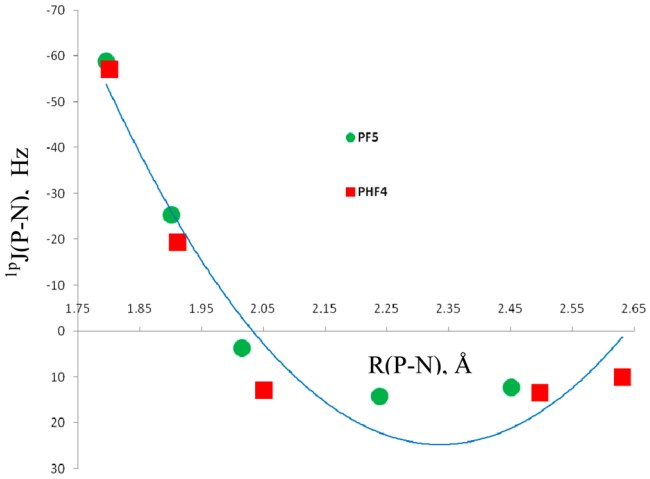

Figure 7. ^{1p}J(P−N) versus the P−N distance for complexes F_5P:N-base and HF_4P:N-base.

Hz, respectively, which more closely resemble the positive values in complexes of the other acids with NC^-. Thus, the electronic effects of the four equatorial F atoms must play a prime role in determining the signs and magnitudes of ^{1p}J(P−N) in complexes of PF_5 and PHF_4 with nitrogen bases.

Table 5 also reports ^{1p}J(P−N) values for the complexes H_4FP:N-base and H_2F_3P:N-base. In contrast to complexes with F_5P:N-base and HF_4P:N-base, these complexes have positive values of ^{1p}J(P−N) with the strongest bases NC^- and NCLi. ^{1p}J(P−N) is also positive for H_4FP:NP but negative for the remaining complexes. The variation of ^{1p}J(P−N) with distance is shown in Figure 8 and indicates that PH_4F discriminates among all of the bases, while PH_2F_3 discriminates only the two strongest bases. These complexes share the feature of a linear F_{ax}−P···N alignment. The correlation coefficient of the trendline for the entire set of data points in Figure 8 is 0.863, while that for the complexes H_4FP:N-base is 0.978. The distance dependence of ^{1p}J(P−N) for the complexes with two F atoms in equatorial positions can be seen to be quite different from that for the complexes with four equatorial F atoms. From a sum-over-states perspective, the signs and magnitudes of contributions from excited states which couple to the ground state through the Fermi-contact operator must be influenced by the electronic effects of the four F atoms in the equatorial plane. These effects are quite different from those arising from either two or no F atoms in equatorial positions.

The final set of complexes are H_5P:N-base and H_3F_2P:N-base, which have H_{ax}−P···N linear. The variation of ^{1p}J(P−N) with the P−N distance is similar to that for the set H_4FP:N-base and H_2F_3P:N-base. However, positive ^{1p}J(P−N) are found

dx.doi.org/10.1021/jp509353a | J. Phys. Chem. A 2014, 118, 10144−10154

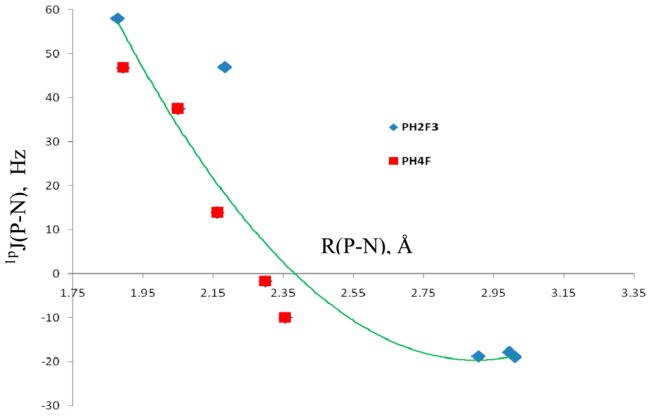

Figure 8. ^{1p}J(P−N) versus the P−N distance for complexes H_4FP:N-base and H_2F_3P:N-base.

only for H_5P:NC^- and H_3F_2P:NC^-, with values of 53 and 74 Hz, respectively. The remaining complexes have negative values of ^{1p}J(P−N), which range from −1 to −17 Hz, with the values for the PH_5 complexes being less negative than those for PH_3F_2. The single trendline shown in Figure 9 has a correlation coefficient of 0.994.

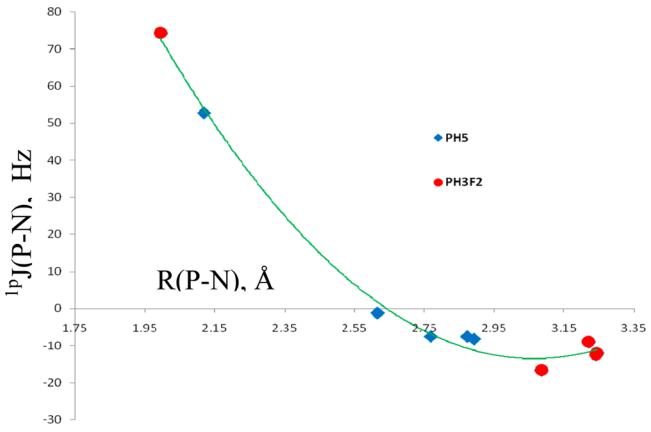

Figure 9. ^{1p}J(P−N) versus the P−N distance for complexes H_5P:N-base and H_3F_2P:N-base.

Table 6 presents the P−F_{ax} distances and coupling constants ^1J(P−F_{ax}). The P−F_{ax} distances in complexes with F_{ax}−P···N linear with a fixed base increase in the order PF_5 < PH_2F_3 < PH_4F, although the absolute values of ^1J(P−F_{ax}) decrease in the order PH_2F_3 > PF_5 > PH_4F. The relationship between ^1J(P−F_{ax}) and the P−F_{ax} distance can be seen in Figure 10. For a fixed acid, the absolute value of ^1J(P−F_{ax}) increases in going from the strongest to the weakest base with one exception. ^1J(P−F_{ax}) values are best discriminated in complexes with PF_5 as the acid, as is readily seen in Figure 10. The linear trendlines for the complexes F_5P:N-base, H_2F_3P:N-base, and H_4FP:N-base have correlation coefficients R^2 of 0.995, 0.941, and 0.985, respectively.

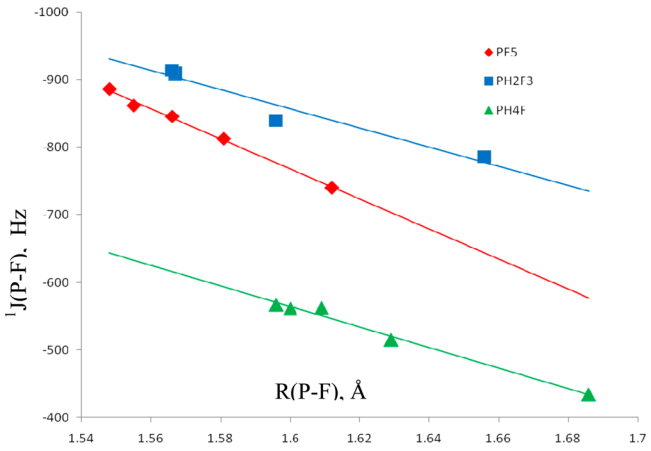

Figure 10. ^1J(P−F_{ax}) versus the P−F_{ax} distance for complexes F_5P:N-base, H_2F_3P:N-base, and H_4FP:N-base.

Table 6 also presents the P−H_{ax} distances and coupling constants ^1J(P−H_{ax}), and Figure 11 presents plots of these variables. In these complexes with H_{ax}−P···N linear, the P−H_{ax} distances for a fixed base decrease in the order PH_5 > PH_3F_2 > PHF_4, although the distance changes are small. Nevertheless, the coupling constants ^1J(P−H_{ax}) increase dramatically with decreasing P−H_{ax} distance. In contrast, for a fixed acid, changes in the P−H_{ax} distances are negligible for the bases NP, NCH, and NCF, and ^1J(P−H_{ax}) values for complexes with these bases are nearly superimposable in Figure 11. Only in complexes with the stronger bases NC^- and NCLi are ^1J(P−H_{ax}) values distinct. The correlation coefficients R^2 for HF_4P:N-base, H_3F_2P:N-base, and H_5P:N-base are 0.886, 0.988, and 0.979, respectively. The reduced correlation coefficient for HF_4P:N-base is a result of the small variations in both P−H_{ax} distances and ^1J(P−H_{ax}) values.

Table 6. MP2/aug′-cc-pVTZ Distances [R(P−F_{ax}) and R(P−H_{ax}), Å][a] and Coupling Constants [^1J(P−F_{ax}) and ^1J(P−H_{ax}), Hz] in Complexes $H_nF_{5-n}P$:N-Base

	R(P−F_{ax})/^1J(P−F_{ax})				
acid/base	NC^-	NCLi	NP	NCH	NCF
PF_5	1.612/−739.8	1.581/−812.4	1.566/−846.3	1.555/−861.5	1.548/−886.1
PH_2F_3	1.656/−785.6	1.596/−838.7	1.567/−906.5	1.567/−910.0	1.566/−913.8
PH_4F	1.686/−434.1	1.629/−515.0	1.609/−562.3	1.600/−561.2	1.596/−567.2
	R(P−H_{ax})/^1J(P−H_{ax})				
acid/base	NC^-	NCLi	NP	NCH	NCF
PHF_4	1.394/794.5	1.385/805.8	1.381/807.0	1.379/811.5	1.378/818.9
PH_3F_2	1.426/304.5	1.389/575.2	1.388/622.6[b]	1.388/610.5	1.388/614.0
PH_5	1.441/193.7	1.407/288.3	1.402/319.1	1.401/327.1	1.400/331.1

[a] P−F_{ax} and P−H_{ax} refer to the axial F and H atoms. [b] The equilibrium complex with C_s symmetry. The C_{2v} complex has a P−H_{ax} distance of 1.388 Å and ^1J(P−H_{ax}) equal to 604.5 Hz.

dx.doi.org/10.1021/jp509353a | J. Phys. Chem. A 2014, 118, 10144−10154

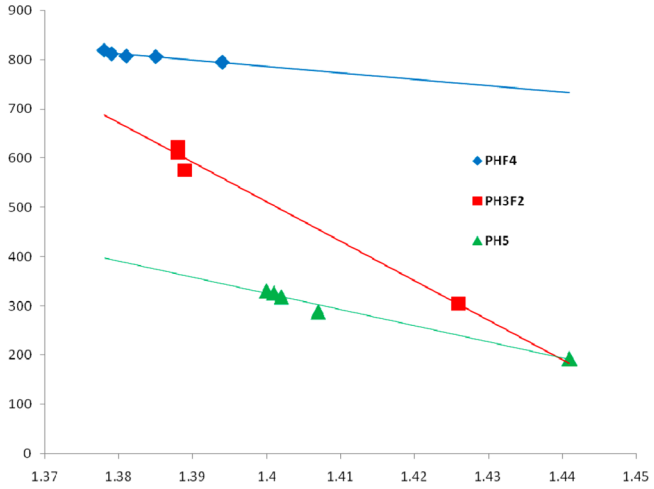

Figure 11. $^{1}J(P-H_{ax})$ versus the $P-H_{ax}$ distance for complexes HF_4P:N-base, H_3F_2P:N-base, and H_5P:N-base.

CONCLUSIONS

Ab initio MP2/aug′-cc-pVTZ calculations have been carried out on the pnicogen-bonded complexes $H_nF_{5-n}P$:N-base for n = 0−5 and nitrogen bases NC^-, NCLi, NP, NCH, and NCF. The following statements are supported by the results of this study.

(1) The structures of $H_nF_{5-n}P$:N-base complexes have either C_{4v} or C_{2v} symmetry, except for H_3F_2P:NP, which has C_s symmetry. P−N distances vary dramatically from 1.80 to 3.24 Å, while $F_{ax}-P-F_{eq}$ angles in complexes with PF_5 vary from 91° at short P−N distances to 100° at long distances. Thus, this angle approaches the $F_{ax}-P-F_{eq}$ angle of 102° computed for the Berry pseudorotation transition structure which interconverts axial and equatorial F atoms of PF_5. The computed distances and $F_{ax}-P-F_{eq}$ angles in complexes F_5P:N-base are consistent with experimental CSD data for complexes of PF_5 with nitrogen bases.

(2) The interaction energies of neutral complexes vary from −13 to −193 kJ·mol^{-1}. This range is extended to −391 kJ·mol^{-1} when the anionic complexes are included. For a fixed acid, the interaction energies decrease in the order NC^- > NCLi > NP > NCH > NCF.

(3) For a fixed base, there is no single pattern for the variations in distances and interaction energies, which suggests that there are multiple factors that influence these properties. These include the number of F atoms in equatorial positions, whether $F_{ax}-P\cdots N$ or $H_{ax}-P\cdots N$ is linear, and the electron-donating ability of the nitrogen base. With respect to the acid, the dominant factor appears to be the presence of four equatorial F atoms, followed by an $F_{ax}-P\cdots N$ linear alignment rather than $H_{ax}-P\cdots N$. Thus, the PH_nF_{5-n} acids may be grouped into pairs (PF_5, PHF_4) with four equatorial F atoms, then (PH_4F, PH_2F_3) with $F_{ax}-P\cdots N$ linear, and then (PH_3F_2, PH_5) with $H_{ax}-P\cdots N$ linear.

(4) Charge transfer from the N lone pair to the σ^* $P-A_{ax}$ orbital stabilizes $H_nF_{5-n}P$:N-base complexes. Complexes with four equatorial F atoms also have additional charge-transfer interactions, from the N lone pair to the σ^* $P-F_{eq}$ orbitals. The total charge-transfer energies correlate with the interaction energies of these complexes.

(5) Spin−spin coupling constants $^{1p}J(P-N)$ for (PF_5, PHF_4) complexes with nitrogen bases are negative for the strongest bases NC^- and NCLi, but then change sign and become positive for complexes with the remaining bases. In contrast, complexes of (PH_4F, PH_2F_3) with NC^- and NCLi and H_4FP:NP have positive $^{1p}J(P-N)$ values but negative values for the remaining bases. Complexes with (PH_5, PH_3F_2) as the acids have negative values of $^{1p}J(P-N)$ only in the anionic complexes with NC^-.

(6) Values of $^{1}J(P-F_{ax})$ for complexes of each of the acids PF_5, PH_2F_3, and PH_4F with the nitrogen bases correlate with the $P-F_{ax}$ distance. Similarly, complexes of PHF_4, PH_3F_2, and PH_5 with these same bases have values of $^{1}J(P-H_{ax})$ that correlate with the $P-H_{ax}$ distance.

ASSOCIATED CONTENT

Supporting Information

Geometries, total energies, and molecular graphs of complexes $H_nF_{5-n}P$:N-base; PF_5:N-base complexes found in the CSD database; values of electron densities, Laplacians, and energy densities at bond critical points; components of coupling constants $^{1p}J(P-N)$, $^{1}J(P-F_{ax})$, and $^{1}J(P-H_{ax})$; full refs 58 and 75. This material is available free of charge via the Internet at http://pubs.acs.org.

AUTHOR INFORMATION

Corresponding Authors

*E-mail: jedelbene@ysu.edu. Tel.: +1 330-609-5593.
*E-mail: ibon@iqm.csic.es Tel.: +34 915622900.

Notes

The authors declare no competing financial interest.

ACKNOWLEDGMENTS

This work was carried out with financial support from the Ministerio de Economía y Competitividad (Project CTQ2012-35513-C02-02) and Comunidad Autónoma de Madrid (Project MADRISOLAR2, ref S2009/PPQ1533). Thanks are also given to the Ohio Supercomputer Center and CTI (CSIC) for their continued computational support.

REFERENCES

(1) Klinkhammer, K. W.; Pyykko, P. Ab Initio Interpretation of the Closed-Shell Intermolecular E···E Attraction in Dipnicogen (H_2E-EH_2)$_2$ and Dichalcogen (HE-EH)$_2$ Hydride Model Dimers. *Inorg. Chem.* **1995**, *34*, 4134−4138.

(2) Carré, F.; Chuit, C.; Corriu, R. J. P.; Monforte, P.; Nayyar, N. K.; Reyé, C. Intramolecular Coordination at Phosphorus: Donor-Acceptor Interaction in Three- and Four-Coordinated Phosphorus Compounds. *J. Organomet. Chem.* **1995**, *499*, 147−154.

(3) Ganesamoorthy, C.; Balakrishna, M. S.; Mague, J. T.; Tuononen, H. M. New Tetraphosphane Ligands {$(X_2P)_2NC_6H_4N(PX_2)_2$} (X = Cl, F, OMe, OC_6H_4OMe-*o*): Synthesis, Derivatization, Group 10 and 11 Metal Complexes and Catalytic Investigations. DFT Calculations on Intermolecular P···P Interactions in Halo-Phosphines. *Inorg. Chem.* **2008**, *47*, 7035−7047.

(4) Moilanen, J.; Ganesamoorthy, C.; Balakrishna, M. S.; Tuononen, H. M. Weak Interactions between Trivalent Pnictogen Centers: Computational Analysis of Bonding in Dimers $X_3E\cdots EX_3$ (E = Pnictogen, X = Halogen). *Inorg. Chem.* **2009**, *48*, 6740−6747.

(5) Sundberg, M. R.; Uggla, R.; Viñas, C.; Teixidor, F.; Paavola, S.; Kivekäs, R. Nature of Intramolecular Interactions in Hypercoordinate C-Substituted 1,2-Dicarba-cloro-dodecaboranes with Short P···P Distances. *Inorg. Chem. Commun.* **2007**, *10*, 713−716.

(6) Murray, J. S.; Lane, P.; Politzer, P. A Predicted New Type of Directional Noncovalent Interaction. *Int. J. Quantum Chem.* **2007**, *107*, 2286−2292.

(7) Zahn, S.; Frank, R.; Hey-Hawkins, E.; Kirchner, B. Pnicogen Bonds: A New Molecular Linker? *Chem.—Eur. J.* **2011**, *17*, 6034−6038.

(8) Scheiner, S. A New Noncovalent Force: Comparison of P···N Interaction with Hydrogen and Halogen Bonds. *J. Chem. Phys.* **2011**, *134*, 094315.
(9) Del Bene, J. E.; Alkorta, I.; Sánchez-Sanz, G.; Elguero, J. ^{31}P-^{31}P Spin-Spin Coupling Constants for Pnicogen Homodimers. *Chem. Phys. Lett.* **2011**, *512*, 184−187.
(10) Del Bene, J. E.; Alkorta, I.; Sánchez-Sanz, G.; Elguero, J. Structures, Energies, Bonding, and NMR Properties of Pnicogen Complexes H_2XP:NXH_2 (X = H, CH_3, NH_2, OH, F, Cl). *J. Phys. Chem. A* **2011**, *115*, 13724−13731.
(11) Del Bene, J. E.; Alkorta, I.; Sánchez-Sanz, G.; Elguero, J. Structures, Binding Energies, and Spin-Spin Coupling Constants of Geometric Isomers of Pnicogen Homodimers $(PHFX)_2$, X = F, Cl, CN, CH_3, NC. *J. Phys. Chem. A* **2012**, *116*, 3056−3060.
(12) Del Bene, J. E.; Sanchez-Sanz, G.; Alkorta, I.; Elguero, J. Homo- and Heterochiral Dimers $(PHFX)_2$, X = Cl, CN, CH_3, NC: To What Extent Do They Differ? *Chem. Phys. Lett.* **2012**, *538*, 14−18.
(13) Del Bene, J. E.; Alkorta, I.; Sánchez-Sanz, G.; Elguero, J. Interplay of F−H···F Hydrogen Bonds and P···N Pnicogen Bonds. *J. Phys. Chem. A* **2012**, *116*, 9205−9213.
(14) Alkorta, I.; Sánchez-Sanz, G.; Elguero, J. Influence of Hydrogen Bonds on the P···P Pnicogen Bond. *J. Chem. Theory Comput.* **2012**, *8*, 2320−2327.
(15) Alkorta, I.; Sánchez-Sanz, G.; Elguero, J.; Del Bene, J. E. Exploring $(NH_2F)_2$, H_2FP:NFH_2, and $(PH_2F)_2$ Potential Surfaces: Hydrogen Bonds or Pnicogen Bonds? *J. Phys. Chem. A* **2013**, *117*, 183−191.
(16) Del Bene, J. E.; Alkorta, I.; Sánchez-Sanz, G.; Elguero, J. Phosphorus as a Simultaneous Electron-Pair Acceptor in Intermolecular P···N Pnicogen Bonds and Electron-Pair Donor To Lewis Acids. *J. Phys. Chem. A* **2013**, *117*, 3133−3141.
(17) Grabowski, S. J.; Alkorta, I.; Elguero, J. Complexes between Dihydrogen and Amine, Phosphine, and Arsine Derivatives. Hydrogen Bond Versus Pnictogen Interaction. *J. Phys. Chem. A* **2013**, *117*, 3243−3251.
(18) Sánchez-Sanz, G.; Alkorta, I.; Trujillo, C.; Elguero, J. Intramolecular Pnicogen Interactions In PHF-$(CH_2)_n$-PHF (n = 2−6) Systems. *ChemPhysChem.* **2013**, *14*, 1656−1665.
(19) Alkorta, I.; Elguero, J.; Del Bene, J. E. Pnicogen-Bonded Cyclic Trimers $(PH_2X)_3$ with X = F, Cl, OH, NC, CN, CH_3, H, and BH_2. *J. Phys. Chem. A* **2013**, *117*, 4981−4987.
(20) Del Bene, J. E.; Alkorta, I.; Elguero, J. Characterizing Complexes with Pnicogen Bonds Involving sp^2 Hybridized Phosphorus Atoms: $(H_2C{=}PX)_2$ with X = F, Cl, OH, CN, NC, CCH, H, CH_3, and BH_2. *J. Phys. Chem. A* **2013**, *117*, 6893−6903.
(21) Alkorta, I.; Elguero, J.; Del Bene, J. E. Pnicogen Bonded Complexes of PO_2X (X = F, Cl) with Nitrogen Bases. *J. Phys. Chem. A* **2013**, *117*, 10497−10503.
(22) Bauzá, A.; Alkorta, I.; Frontera, A.; Elguero, J. On the Reliability of Pure and Hybrid DFT Methods for the Evaluation of Halogen, Chalcogen, and Pnicogen Bonds Involving Anionic and Neutral Electron Donors. *J. Chem. Theory Comput.* **2013**, *9*, 5201−5210.
(23) Del Bene, J. E.; Alkorta, I.; Elguero, J. Properties of Complexes $H_2C{=}(X)P$:PXH_2, for X = F, Cl, OH, CN, NC, CCH, H, CH_3, and BH_2: P···P Pnicogen Bonding at σ-Holes and π-Holes. *J. Phys. Chem. A* **2013**, *117*, 11592−11604.
(24) Alkorta, I.; Elguero, J.; Solimannejad, M. Single Electron Pnicogen Bonded Complexes. *J. Phys. Chem. A* **2014**, *118*, 947−953.
(25) Del Bene, J. E.; Alkorta, I.; Elguero, J. σ-σ and σ-π Pnicogen Bonds In Complexes H_2XP:PCX, for X = F, Cl, OH, NC, CN, CCH, CH_3, and H. *Theor. Chem. Acc.* **2014**, *133*, 1464−1/9.
(26) Del Bene, J. E.; Alkorta, I.; Elguero, J. Influence of Substituent Effects on the Formation of P···Cl Pnicogen Bonds or Halogen Bonds. *J. Phys. Chem. A* **2014**, *118*, 2360−2366.
(27) Del Bene, J. E.; Alkorta, I.; Elguero, J. Pnicogen-Bonded Anionic Complexes. *J. Phys. Chem. A* **2014**, *118*, 3386−3392.
(28) Sánchez-Sanz, G.; Trujillo, C.; Alkorta, I.; Elguero, J. Intramolecular Pnicogen Interactions in Phosphorus and Arsenic Analogues of Proton Sponges. *Phys. Chem. Chem. Phys.* **2014**, *16*, 15900−15909.
(29) Dobado, J. A.; Martínez-García, H.; Molina Molina, J.; Sundberg, M. R. Chemical Bonding in Hypervalent Molecules Revised. Application of the Atoms in Molecules Theory to Y_3X and Y_3XZ (Y = H or CH_3; X = N, P or As; Z = O or S) Compounds. *J. Am. Chem. Soc.* **1998**, *120*, 8461−8471.
(30) Lo, Q.-Z.; Li, R.; Liu, X.-F.; Li, W.-Z.; Cheng, J.-B. Concerted Interaction between Pnicogen and Halogen Bonds in XCl−FH_2P−NH_3 (X = F, OH, CN, NC, and FCC). *ChemPhysChem.* **2012**, *13*, 1205−1212.
(31) Adhikari, U.; Scheiner, S. Effects of Carbon Chain Substituents on the P···N Noncovalent Bond. *Chem. Phys. Lett.* **2012**, *536*, 30−33.
(32) An, X.-L.; Li, R.; Li, Q.-Z.; Liu, X.-F.; Li, W.-Z.; Cheng, J.-B. Substitution, Cooperative, and Solvent Effects on π Pnicogen Bonds in the FH_2P and FH_2As Complexes. *J. Mol. Model.* **2012**, *18*, 4325−4332.
(33) Li, Q.-Z.; Li, R.; Liu, X.-F.; Li, W.-Z.; Cheng, J.-B. Pnicogen-Hydride Interaction between FH_2X (X = P and As) and HM (M = ZnH, BeH, MgH, Li, and Na). *J. Phys. Chem. A* **2012**, *116*, 2547−2553.
(34) Adhikari, U.; Scheiner, S. Substituent Effects On Cl···N, S···N, and P···N Noncovalent Bonds. *J. Phys. Chem. A* **2012**, *116*, 3487−3497.
(35) Bauzá, A.; Quiñonero, D.; Deyà, P. M.; Frontera, A. Pnicogen-π Complexes: Theoretical Study and Biological Implications. *Phys. Chem. Chem. Phys.* **2012**, *14*, 14061−14066.
(36) Scheiner, S. The Pnicogen Bond: Its Relation to Hydrogen, Halogen, and Other Noncovalent Bonds. *Acc. Chem. Res.* **2013**, *46*, 280−288.
(37) Scheiner, S. Sensitivity of Noncovalent Bonds to Intermolecular Separation: Hydrogen, Halogen, Chalcogen, and Pnicogen Bonds. *CrystEngComm* **2013**, *15*, 3119−3124.
(38) Scheiner, S. Detailed Comparison of the Pnicogen Bond with Chalcogen, Halogen, and Hydrogen Bonds. *Int. J. Quantum Chem.* **2013**, *113*, 1609−1620.
(39) Bauzá, A.; Quiñonero, D.; Deyà, P. M.; Frontera, A. Is the Use of Diffuse Functions Essential for the Properly Description of Noncovalent Interactions Involving Anions? *J. Phys. Chem. A* **2013**, *117*, 2651−2655.
(40) Adhikari, U.; Scheiner, S. Magnitude and Mechanism of Charge Enhancement of CH···O Hydrogen Bonds. *J. Phys. Chem. A* **2013**, *117*, 10551−10562.
(41) Eskandari, K.; Mahmoodabadi, N. Pnicogen Bonds: A Theoretical Study Based on the Laplacian of Electron Density. *J. Phys. Chem. A* **2013**, *117*, 13018−13024.
(42) Solimannejad, M.; Gholipour, A. Revealing Substituent Effects On the Concerted Interaction of Pnicogen, Chalcogen, and Halogen Bonds in Substituted *s*-Triazine Ring. *Struct. Chem.* **2013**, *24*, 1705−1711.
(43) Cavallo, G.; Metrangolo, P.; Pilati, T.; Resnati, G.; Terraneo, G. Naming Interactions from the Electrophilic Site. *Cryst. Growth Des.* **2014**, *14*, 2697−2702.
(44) Bauzá, A.; Ramis, F.; Frontera, A. A Combined Theoretical and Cambridge Structural Database Study of π-Hole Pnicogen Bonding Complexes between Electron Rich Molecules and Both Nitro Compounds and Inorganic Bromides (YO_2Br, Y = N, P, and As). *J. Phys. Chem. A* **2014**, *118*, 2827−2834.
(45) George, J.; Deringer, V. L.; Dronskowski, R. Cooperativity of Halogen, Chalcogen, and Pnictogen Bonds in Infinite Molecular Chains by Electronic Structure Theory. *J. Phys. Chem. A* **2014**, *118*, 3193−3200.
(46) Clark, T.; Hennemann, M.; Murray, J. S.; Politzer, P. Halogen Bonding: The σ-Hole. *J. Mol. Model.* **2007**, *13*, 291−296.
(47) Kolár, M. H.; Carloni, P.; Hobza, P. Statistical Analysis of σ-Holes: A Novel Complementary View on Halogen Bonding. *Phys. Chem. Chem. Phys.* **2014**, *16*, 19111−19114.
(48) Politzer, P.; Murray, J. S.; Janjić, G. V.; Zarić, S. D. σ-Hole Interactions of Covalently-Bonded Nitrogen, Phosphorus and Arsenic: A Survey of Crystal Structures. *Crystals* **2014**, *4*, 12−31.

(49) Alkorta, I.; Sánchez-Sanz, G.; Elguero, J.; Del Bene, J. E. Pnicogen Bonds between X=PH_3 (X = O, S, NH, CH_2) and Phosphorus and Nitrogen Bases. *J. Phys. Chem. A* **2014**, *118*, 1527−1537.
(50) Deiters, J. A.; Holmes, R. R. Ab Initio Treatment of a Phosphorus Coordinate, Trigonal Bipyramidal to Pentafluoride-Pyridine Reaction Square Pyramidal to Octahedral. *Phosphorus, Sulfur Silicon Relat. Elem.* **1997**, *123*, 329−340.
(51) Pople, J. A.; Binkley, J. S.; Seeger, R. Theoretical Models Incorporating Electron Correlation. *Int. J. Quantum Chem., Quantum Chem. Symp.* **1976**, *10*, 1−19.
(52) Krishnan, R.; Pople, J. A. Approximate Fourth-Order Perturbation Theory of the Electron Correlation Energy. *Int. J. Quantum Chem.* **1978**, *14*, 91−100.
(53) Bartlett, R. J.; Silver, D. M. Many-Body Perturbation Theory Applied to Electron Pair Correlation Energies. I. Closed-Shell First-Row Diatomic Hydrides. *J. Chem. Phys.* **1975**, *62*, 3258−3268.
(54) Bartlett, R. J.; Purvis, G. D. Many-Body Perturbation Theory, Coupled-Pair Many-Electron Theory, and the Importance of Quadruple Excitations for the Correlation Problem. *Int. J. Quantum Chem.* **1978**, *14*, 561−581.
(55) Del Bene, J. E. Proton Affinities of Ammonia, Water, and Hydrogen Fluoride and Their Anions: A Quest for the Basis-Set Limit Using the Dunning Augmented Correlation-Consistent Basis Sets. *J. Phys. Chem.* **1993**, *97*, 107−110.
(56) Dunning, T. H. Gaussian Basis Sets for Use in Correlated Molecular Calculations. I. The Atoms Boron through Neon and Hydrogen. *J. Chem. Phys.* **1989**, *90*, 1007−1023.
(57) Woon, D. E.; Dunning, T. H. Gaussian Basis Sets for Use in Correlated Molecular Calculations. V. Core-Valence Basis Sets for Boron through Neon. *J. Chem. Phys.* **1995**, *103*, 4572−4585.
(58) Frisch, M. J.; Trucks, G. W.; Schlegel, H. B.; Scuseria, G. E.; Robb, M. A.; Cheeseman, J. R.; Scalmani, G.; Barone, V.; Mennucci, B.; Petersson, G. A. et al. *Gaussian 09*, revision D.01;Gaussian, Inc.: Wallingford, CT, 2009.
(59) Bader, R. F. W. A Quantum Theory of Molecular Structure and Its Applications. *Chem. Rev. (Washington, DC, U.S.)* **1991**, *91*, 893−928.
(60) Bader, R. F. W. *Atoms in Molecules, A Quantum Theory*; Oxford University Press, Oxford, U.K., 1990.
(61) Popelier, P. L. A. *Atoms In Molecules. An Introduction*; Prentice Hall: Harlow, England, 2000.
(62) Matta, C. F.; Boyd, R. J. *The Quantum Theory of Atoms in Molecules: From Solid State to DNA and Drug Design*; Wiley-VCH: Weinheim, Germany, 2007.
(63) Silvi, B.; Savin, A. Classification of Chemical Bonds Based on Topological Analysis of Electron Localization Functions. *Nature (London, U.K.)* **1994**, *371*, 683−686.
(64) Keith, T. A. *AIMAll*, version 11.08.23; TK Gristmill Software: Overland Park, KS, 2011. aim.tkgristmill.com.
(65) Noury, S.; Krokidis, X.; Fuster, F.; Silvi, B. *TopMoD Package*, 1997
(66) Rozas, I.; Alkorta, I.; Elguero, J. Behavior of Ylides Containing N, O, and C Atoms As Hydrogen Bond Acceptors. *J. Am. Chem. Soc.* **2000**, *122*, 11154−11161.
(67) Reed, A. E.; Curtiss, L. A.; Weinhold, F. Intermolecular Interactions from a Natural Bond Orbital, Donor-Acceptor Viewpoint. *Chem. Rev. (Washington, DC, U.S.)* **1988**, *88*, 899−926.
(68) Glendening, E. D.; Badenhoop, J. K.; Reed, A. E.; Carpenter, J. E.; Bohmann, J. A.; Morales, C. M.; Landis, C. R.; Weinhold, F. *NBO 6.0*; University of Wisconsin: Madison, WI, 2013.
(69) Becke, A. D. Density-Functional Thermochemistry. III. The Role of Exact Exchange. *J. Chem. Phys.* **1993**, *98*, 5648−5652.
(70) Lee, C.; Yang, W.; Parr, R. G. Development of the Colle−Salvetti Correlation-Energy Formula into a Functional of the Electron Density. *Phys. Rev. B: Condens. Matter Mater. Phys.* **1988**, *37*, 785−789.
(71) Perera, S. A.; Nooijen, M.; Bartlett, R. J. Electron Correlation Effects on the Theoretical Calculation of Nuclear Magnetic Resonance Spin−Spin Coupling Constants. *J. Chem. Phys.* **1996**, *104*, 3290−3305.
(72) Perera, S. A.; Sekino, H.; Bartlett, R. J. Coupled−Cluster Calculations of Indirect Nuclear Coupling Constants: The Importance of Non-Fermi Contact Contributions. *J. Chem. Phys.* **1994**, *101*, 2186−2196.
(73) Schäfer, A.; Horn, H.; Ahlrichs, R. Fully Optimized Contracted Gaussian Basis Sets for Atoms Li to Kr. *J. Chem. Phys.* **1992**, *97*, 2571−2577.
(74) Del Bene, J. E.; Elguero, J.; Alkorta, I.; Yáñez, M.; Mó, O. An Ab Initio Study of $^{15}N-^{11}B$ Spin Spin Coupling Constants for Borazine and Selected Derivatives. *J. Phys. Chem. A* **2006**, *110*, 9959−9966.
(75) Stanton, J. F.; Gauss, J.; Watts, J. D.; Nooijen, M.; Oliphant, N.; Perera, S. A.; Szalay, P. S.; Lauderdale, W. J.; Gwaltney, S. R.; Beck, S. et al. *ACES II*; University of Florida: Gainesville, Fl.
(76) Hansen, K. W.; Bartell, L. S. Electron Diffraction Study of the Structure of PF_5. *Inorg. Chem.* **1965**, *4*, 1775−1776; Structure and Bonding in CH_3PF_4 and $(CH_3)_2PF_3$: An Electron Diffraction Study. *Inorg. Chem.* **1965**, *4*, 1777−1782.
(77) Gutowsky, H. S.; McCall, D. W.; Slichter, C. P. Nuclear Magnetic Resonance Multiplets in Liquids. *J. Chem. Phys.* **1953**, *21*, 279−292.
(78) Eisenhut, M.; Mitchell, H. L.; Traficante, D. D.; Kaufman, R. J.; Deutch, J. M.; Whitesides, G. M. Pseudorotation in XPF_4. *J. Am. Chem. Soc.* **1974**, *96*, 5385−5397.
(79) Berry, R. S. Correlation of Rates of Intramolecular Tunneling Processes, with Application to Some Group V Compounds. *J. Chem. Phys.* **1960**, *32*, 933−938.
(80) Selig, H.; Holloway, J. H.; Tyson, J.; Claassen, H. H. Raman Spectra of AsF_5 and VF_5 and Force Constants for PF_5, AsF_5, and VF_5. *J. Chem. Phys.* **1970**, *53*, 2559−2564.
(81) Wasada, H.; Hirao, K. Theoretical Study of the Reactions of Pentacoordinated Trigonal Bipyramidal Phosphorus Compounds: PH_5, PF_5, PF_4H, PF_3H_2, PF_4CH_3, $PF_3(CH_3)_2$, $P(O_2C_2H_4)H_3$, $P(OC_3H_6)H_3$, and $PO_5H_4^-$. *J. Am. Chem. Soc.* **1992**, *114*, 16−27.
(82) Daula, C.; Friouda, M.; Schafera, O.; Sellonib, A. Non-Empirical Dynamical DFT Calculation of the Berry Pseudorotation of PF_5. *Chem. Phys. Lett.* **1996**, *262*, 74−79.
(83) Burenin, A. V. Qualitative Quantum Dynamics with Allowance for Berry Pseudorotation in XPF_4 and PF_5 Molecules: II. The PF_5 Molecule. *Opt. Spectrosc.* **2002**, *92*, 45−52.
(84) Caligiana, A.; Aquilanti, V.; Burcl, R.; Handy, N. C.; Tew, D. P. Anharmonic Frequencies and Berry Pseudorotation Motion in PF_5. *Chem. Phys. Lett.* **2003**, *369*, 335−344.
(85) Raynaud, C.; Maron, L.; Daudey, J. P.; Jolibois, F. Berry Pseudorotation Mechanism for the Interpretation of the ^{19}F NMR Spectrum in PF_5 by Ab Initio Molecular Dynamics Simulations. *ChemPhysChem* **2006**, *7*, 407−413.
(86) Cass, M. E.; Hii, K. H.; Rzepa, H. S. Mechanisms That Interchange Axial and Equatorial Atoms in Fluxional Processes: Illustration of the Berry Pseudorotation, the Turnstile, and the Lever Mechanisms Via Animation of Transition State Normal Vibrational Modes. *J. Chem. Educ.* **2006**, *83*, 336.
(87) Couzijn, E. P. A.; Slootweg, J. C.; Ehlers, A. W.; Lammertsma, K. Stereomutation of Pentavalent Compounds: Validating the Berry Pseudorotation, Redressing Ugi's Turnstile Rotation, and Revealing the Two- and Three-Arm Turnstiles. *J. Am. Chem. Soc.* **2010**, *132*, 18127−18140.
(88) Moberg, C. Stereomutation in Trigonal-Bipyramidal Systems: A Unified Picture. *Angew. Chem., Int. Ed.* **2011**, *50*, 10290−10292.
(89) Allen, F. H. The Cambridge Structural Database: A Quarter of a Million Crystal Structures and Rising. *Acta Crystallogr.* **2002**, *B58*, 380−388.
(90) Knop, O.; Boyd, R. J.; Choi, S. C. Sulfur-Sulfur Bond Lengths, or Can a Bond Length Be Estimated from a Single Parameter? *J. Am. Chem. Soc.* **1988**, *110*, 7299−7301.
(91) Gibbs, G. V.; Hill, F. C.; Boisen, M. B.; Downs, R. T. Power Law Relationships between Bond Length, Bond Strength and Electron Density Distributions. *Phys. Chem. Minerals* **1998**, *25*, 585−590.

(92) Alkorta, I.; Barrios, L.; Rozas, I.; Elguero, J. Comparison of Models to Correlate Electron Density at the Bond Critical Point and Bond Distance. . *Mol. Struct.: THEOCHEM* **2000**, *496*, 131−137.
(93) Knop, O.; Rankin, K. N.; Boyd, R. J. Coming to Grips with N−H···N Bonds. 1. Distance Relationships and Electron Density at the Bond Critical Point. *J. Phys. Chem. A* **2001**, *105*, 6552−6566.
(94) Knop, O.; Rankin, K. N.; Boyd, R. J. Coming to Grips with N−H···N Bonds. 2. Homocorrelations between Parameters Deriving from the Electron Density at the Bond Critical Point. *J. Phys. Chem. A* **2003**, *107*, 272−284.
(95) Espinosa, E.; Alkorta, I.; Elguero, J.; Molins, E. From Weak to Strong Interactions: A Comprehensive Analysis of the Topological and Energetic Properties of the Electron Density Distribution Involving X−H···F−Y Systems. *J. Chem. Phys.* **2002**, *117*, 5529−5542.
(96) Alkorta, I.; Elguero, J. Fluorine−Fluorine Interactions: NMR and AIM Analysis. *Struct. Chem.* **2004**, *15*, 117−120.
(97) Tang, T. H.; Deretey, E.; Jensen, S. J. K.; Csizmadia, I. G. Hydrogen Bonds: Relation between Lengths and Electron Densities at Bond Critical Points. *Eur. Phys. J. D* **2006**, *37*, 217−222.
(98) Mata, I.; Alkorta, I.; Molins, E.; Espinosa, E. Universal Features of the Electron Density Distribution in Hydrogen-Bonding Regions: A Comprehensive Study Involving H···X (X = H, C, N, O, F, S, Cl, π) Interactions. *Chem.—Eur. J.* **2010**, *16*, 2442−2452.
(99) Sanchez, M.; Provasi, P. F.; Aucar, G. A.; Alkorta, I.; Elguero, J. Theoretical Study of HCN and HNC Neutral and Charged Clusters. *J. Phys. Chem. B* **2005**, *109*, 18189−18194.
(100) Alkorta, I.; Zborowski, K.; Elguero, J.; Solimannejad, M. Theoretical Study of Dihydrogen Bonds between $(XH)_2$, X = Li, Na, BeH, and MgH, and Weak Hydrogen Bond Donors (HCN, HNC, and HCCH). *J. Phys. Chem. A* **2006**, *110*, 10279−10286.